scientific reports

Check for updates

OPEN

Synthesis of silver nanoparticles using *Plantago lanceolata* extract and assessing their antibacterial and antioxidant activities

Muhammad Zahir Shah[1], Zheng-Hui Guan[1]✉, Ala Ud Din[2]✉, Amjad Ali[3], Ata Ur Rehman[2], Kashif Jan[2], Shah Faisal[4], Shah Saud[5,6]✉, Muhammad Adnan[7], Fazli Wahid[7], Saud Alamri[8], Manzer H. Siddiqui[8], Shamsher Ali[9], Wajid Nasim[10], Hafiz Mohsin Hammad[11] & Shah Fahad[12,13]✉

Silver nanoparticles (Ag. NPs) have shown a biological activity range, synthesized under different environment-friendly approaches. Ag. NPs were synthesized using aqueous crude extract (ACE) isolated from *Plantago lanceolata*. The ACE and Ag. NPs were characterized and assessed their biological and antioxidant activities. The existence of nanoparticles (NPs) was confirmed by color shift, atomic force microscopy (AFM) and UV–Vis's spectroscopy. The FT-IR analysis indicated the association of biomolecules (phenolic acid and flavonoids) to reduce silver (Ag^+) ions. The SEM study demonstrated a sphere-shaped and mean size in the range of 30 ± 4 nm. The EDX spectrum revealed that the Ag. NPs were composed of 54.8% Ag with 20 nm size as identified by SEM and TEM. AFM has ended up being exceptionally scrutiny in deciding morphological elements and the distance across of Ag. NPs in the scope of 23–50 nm. The TEM image showed aggregations of NPs and physical interaction. Ag. NPs formation also confirmed by XPS, DRS and BET studies. Ag. NPs showed efficient activity as compared to ACE, and finally, the bacterial growth was impaired by biogenic NPs. The lethal dose (LD_{50}) of Ag. NPs against *Agrobacterium tumefaciens*, *Proteus vulgaris*, *Staphylococcus aureus*, and *Escherichia coli* were 45.66%, 139.71%, 332.87%, and 45.54%, with IC50 (08.02 ± 0.68), (55.78 ± 1.01), (12.34 ± 1.35) and (11.28 ± 1.42) respectively, suppressing the growth as compared to ACE. The antioxidant capacity, i.e., 2,2-diphenyl-1-picrylhydrazyl (DPPH) of Ag. NPs were assayed. ACE and Ag. NPs achieved peak antioxidant capacity of 62.43 ± 2.4 and 16.85 ± 0.4 μg mL^{-1}, compared to standard (60.60 ± 1.1 at 100 μg mL^{-1}) with IC_{50} (369.5 ± 13.42 and 159.5 ± 10.52 respectively). Finally, the Ag. NPs synthesized by *P. lanceolata* extract have an excellent source of bioactive natural products (NP). Outstanding antioxidant, antibacterial activities have been shown by NPs and can be used in various biological techniques in future research.

RETRACTED ARTICLE

[1]Key Laboratory of Synthetic and Natural Functional Molecule Chemistry of Ministry of Education, Department of Chemistry and Materials Science, Northwest University, Xi'an 710127, China. [2]Department of Chemistry, University of Buner, Buner 17290, Pakistan. [3]School of Environmental and Municipal Engineering, Xi'an University of Architecture and Technology, Xi'an 710051, China. [4]Department of Physics, Riphah International University, Islamabad 46000, Pakistan. [5]Faculty of Tropical AgriSciences, Czech University of Life Sciences Prague, Prague, Czech Republic. [6]Department of Horticulture, Northeast Agricultural University, Harbin, China. [7]Department of Agriculture, University of Swabi, Swabi, Pakistan. [8]Department of Botany and Microbiology, College of Science, King Saud University, Riyadh 11451, Saudi Arabia. [9]Department of Soil and Environmental Sciences, Amir Muhammad Khan Campus Mardan, The University of Agriculture, Peshawar, Khyber Pakhtunkhwa, Pakistan. [10]Department of Agronomy, University College of Agriculture and Environmental Sciences, The Islamia University of Bahawalpur (IUB), Bahawalpur, Pakistan. [11]Department of Agronomy, Muhammad Nawaz Sharif University of Agriculture, Multan 66000, Pakistan. [12]Hainan Key Laboratory for Sustainable Utilization of Tropical Bioresource, College of Tropical Crops, Hainan University, Haikou 570228, China. [13]Department of Agronomy, The University of Haripur, Haripur 22620, Khyber Pakhtunkhwa, Pakistan. ✉email: guanzhj@nwu.edu.cn; allauddin4763@gmail.com; saudhort@gmail.com; shah_fahad80@yahoo.com

Nanoparticles (NP) are synthesized from fauna/flora extracts and elements such as silver (Ag), gold (Au), platinum (Pt), nickel (Ni), zinc (Zn), copper (Cu), and compounds like titanium dioxide (TiO_2), ferrous oxide (FeO), and ferric oxide (Fe_2O_3)[1]. The applications are primarily determined via properties such as size, shape, composition, crystallinity, and structure of the NPs[2,3]. The synthesis and characterization of NPs is an emerging nanotechnology field established over the past two decades due to a wide variety of applications in the areas of chemistry, physics, biology, medicine, textile[4,5], wastewater treatment, and drug delivery[6]. Generally, the synthesis of silver nanoparticles (Ag. NPs) can be modulated by an extensive range of aspects, such as biological substances, temperature, pH, the strength of metal ions, heat, reaction time, and electromagnetic waves[7].

The adaptations and modifications of these factors can therefore regulate and modulate the characteristics of Ag. NPs, including scale, shape, surface load, surface properties, and crystalline nature, as well as bioactivities[8]. The Ag. NPs are also metal-based and have been an acolyte commodity in the arena of micro/nano-nanotechnology. Ag. NPs with annual use of 454 metric tons, primarily for biomedical applications (antibiotic, antimycotic and antiviral medicines), received growing attention among metal NPs[9]. Due to the exceptional features such as their antibacterial, antiviral, antifungal, and anti-inflammatory activities, Ag. NPs gained unlimited attention from scientists[10,11]. It may be used in nanocomposite products, cosmetics, food processing, computer modules, etc. It also has high chemical consistency, excellent biocompatibility, catalytic efficiency, low toxicity, and eco-friendliness compared to other outmoded antibiotics and chemicals. Ag. NPs are also used in diagnosing various acute and chronic diseases, pharmaceutical delivery, electronics, bio-sensing, the food industry, the garment industry, paints, and health supplements[12].

Compared to the same material in the bulk state, nanomaterial sizes ranging from 1 to 100 nm have significant differences in their properties[13]. Various techniques such as Ag ion reduction in an aqueous medium with or without stabilizing agents can synthesize NPs[14], in organic solvents, by thermal decomposition[15], chemical reduction by radiation[16]. In the literature, chemical reduction and photochemical reduction of quashing micelles have also been reported[17,18]. Typically, these approaches are expensive and require hazardous chemicals that can cause biological risks. Biological techniques of preparing Ag NPs using microorganisms[19–21], fungi[22], enzymes[23], and plant extracts have been recommended to substitute chemical and physical methods due to their eco-friendly nature. Synthesis of NPs by using plants or plant extracts is more accessible than other approaches to a significant degree by reducing the elaborate processes of microbial culture maintenance[24–26].

The antimicrobial potential of Ag has been recognized long before[27]. Ag was the third metal the ancient civilizations learned to use after Au and Cu about 4000 BC. Before the invention of antibiotics, Ag was the most significant antimicrobial substance accessible and various forms for preserving foodstuffs[28]. Ag utensils in the kitchen have been prevalent worldwide due to knowledge of antibacterial activities[29]. Plants and microorganisms are now used for NPs synthesis. Natural bioactive compounds, i.e., primary and secondary metabolites, have a wide range of applications. Chemists have been investigating strategies for eliminating harmful compounds and utilizing healthy metabolites[30].

Plantago lanceolata is a perennial medicinal plant belonging to the family *Plantaginaceae* with about 265 species[31]. Other plants such as *Artocarpus heterophyllus*[13], *Sesbania grandiflora*[30], *Prosopis juliflora,* and *Semecarpus anacardium* extracts used for the synthesis of NPs with different metals[32]. Due to its abundance of active secondary metabolites, *P. lanceolata* is used as an herbal plant in many countries. This plant addresses several health issues, including skin problems, like abscesses and pimples[33]. It is also used to treat cancer, embolism, bee bites, Tuberculosis (TB), and other pneumonia-related anomalies. The plant species and other members displayed promising antimicrobial activity against bacteria, fungi, anthelmintic, and other microbes. It has gained a lot of popularity in countries like Turkey and the Indian subcontinent because of its antioxidant and antiviral activities. Infectious diseases like diarrhea, dysentery, and colic malaria can be treated with *P. lanceolata* boiled water extract with honey[34,35].

There are several other reactive chemical metabolites in *P. lanceolata*. Mainly tannins, flavonoids, mucilage, silica, zinc, potassium salts, iridoid glycosides, phenylpropanoid glycoside, acteoside, flavonoids, and phenyl carboxylic acid are found in leaves. Catapol and its precursor aucubin are the most common iridoid glycosides in *P. lanceolata*[36]. *Plantago lanceolata* is widely used to treat blisters, stomach disorders, uterine cancer, pimples, homeostatic, TB, asthma, bronchitis, and diarrhea[37–40]. The secondary metabolites present in the leaves, roots, and bark are responsible for therapeutic potential. *Plantago lanceolata* is local to Europe and Asia, but with a suitable environment, it spread to North America and many other areas[41].

Plantago lanceolata and its other family affiliate are the best source of several active and beneficial metabolites source and used against several diseases from ancient times. Here we synthesized its Ag. NPs with the ACE enhance its potential against the various enzymes and microbes causing diseases. Ag. NPs have an enormous surface area for their activities against their target compared to simple extracts, which play an essential role in Ag. NP synthesis[40]. The aqueous crude extract (ACE) contains many active compounds, such as tannins, terpenes, anthraquinone, sugar, glycosides, phlobatannins, emodin, phenolic acid, flavonoids, and saponins[42]. The reduction of Ag is actively involved in these compounds for NPs synthesis. The current study aims to prepare NPs of low-cost to establish an innovative approach using different fractions of methanolic crude extracts of *P. lanceolata* and compare their antibacterial and antioxidant activity with ACE.

Materials and methods

Plant materials. The *Plantago lanceolata* was collected from the Mansehra (73°20′8.6″E, 34°37′35.99″N), Khyber Pakhtunkhwa, Pakistan (Fig. 1). Before collection, the plant was identified using the standard protocol at the Department of Life Science, Northwest University, Xi'an, China. The plant specimen was given a voucher number (ZH/134), and its leaves were preserved in the herbarium for future reference. The fresh plant was washed with distilled water to remove dust particles and dried in the shade. The plant material was ground into

RETRACTED ARTICLE

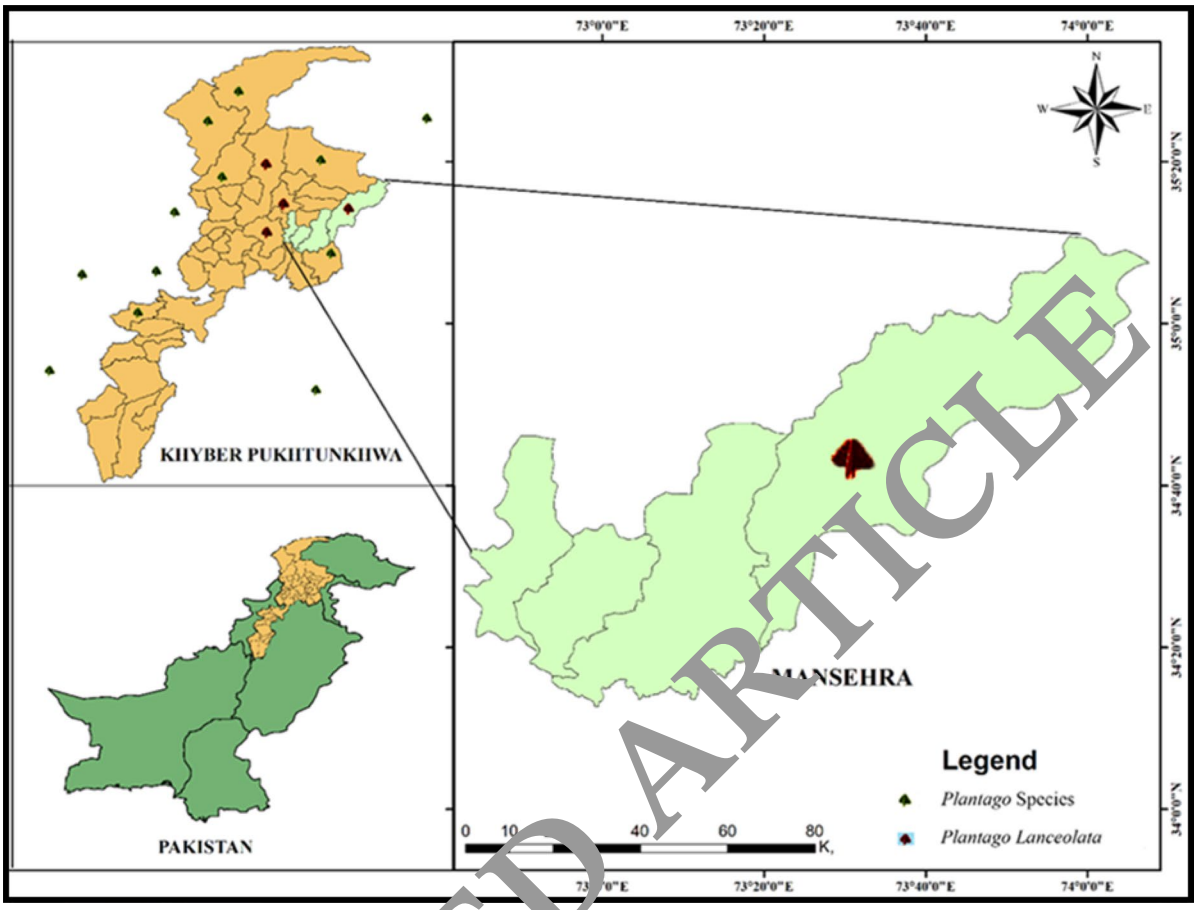

Figure 1. *Plantago* species and *Plantago lanceolata* distribution and collection points map. This map is generated using ArcGis 10.1.2 software. The shape files of the study area (Pakistan, Khyber Pakhtunkhwa, Mansehra) was generated in ArcGis software and then digitized using the location points of the plant species. The official links for this software are:https://www.esri.com/en-us/arcgis/products/arcgis-platform/overview.

RETRACTED ARTICLE

fine particles, and compounds in crude form were extracted with methanol in five conical flasks (1 L each)[36,43]. The crude methanol extract (CME) was filtered, and a rotary evaporator was used to get a thick slurry, stored in the refrigerator at 4 °C. The CME was subdivided on solvent polarity base into n-Hexane, dichloromethane, ethyl acetate, and ACE.

Chemicals. Methanol, Ethanol, Ethyl acetate, *n*-Hexane, Sodium borohydride, DPPH, and other micro-apparatus were purchased from Davidson and Hardy Ltd, Ireland. The King Fahad Medical Research Centre, King Abdul Aziz University, Jeddah, Saudi Arabia, provided bacterial isolates. Deionized water was used in the process for solution preparation, as well as washing and rinsing laboratory equipment. To reduce humidity, the equipment was wrapped in aluminum foil during the tests.

Synthesis and characterization of Ag. NPs. *Synthesis.* Wet chemistry procedures have been used to make nanoparticles, which entailly creating the particles in a solution, drop projecting them onto a substrate, and then extracting the solvent, surfactants, and other components from the particles. Freshly prepared *P. lanceolata*'s extract mixed with 1 Mm AgCl solution (1:9 ratio) at room temperature. Via integrating the freshly made *P. lanceolata* extracts with the freshly made 1 mM $AgCl_2$ solution (1:9 ratio) at room temp, Ag. NPs were synthesized in ice-cold 100 mL deionized water. The ACE stock solution was prepared by mixing 0.1 g of extract into 50 mL of methanol and filtering with Whatman Grade 42. The two stock solutions were combined in a 250 mL flask in various combinations and stirred at room temperature for 4 h. Two solutions were mixed in a 1:1 proportion for the successful synthesis of Ag. NPs[6]. Through incubation, changes in color from pale yellow to reddish-brown were noted in the formation of the NPs. The mixture was then centrifuged at 15,000 rpm for 1 h after incubation to isolate the NPs, and the NPs obtained were air-dried and then further cleaned with deionized water and stored in the incubator. The collected powder (NPs) was stored in the refrigerator for further characterizations[7].

Characterization. UV–Vis spectroscopy and AFM. The NPs obtained were characterized by various measurements, such as UV–Vis spectroscopy, to calculate the maximum wavelength for the quantitative determina-

tion and optical properties. The UV–Vis spectrum of biosynthesized Ag. NPs and ACE were determined using the UV–Vis 1800 spectrophotometer (Shimadzu, Japan). The instrument was operated at room temperature with a 1 nm resolution in the 200, and 600 nm scales[44]. The size and morphology of Ag. NPs were performed by atomic force microscopy (AFM) (AGILENT-N9410A series 5500).

FT-IR analysis. The PerkinElmer FT-IR 1600 spectrophotometer (USA) was used to compare the IR spectra of both Ag. NPs and ACE in the λ range of 400 to 4000 cm^{-1} and 4 cm^{-1}. The universal disc method was followed for the analysis[6].

X-ray diffraction (XRD). Using Rigaku Smart Lab II X-Ray powder diffraction (Japan) with an average source of Cu K $\alpha 1 + K\ \alpha 2$ radiation ($\lambda = 0.15425$ A), the phase units of Ag. XRD measured NPs. The Bragg angles vary from 1° to 60° at a scanning rate of 2° min^{-1} using (Eq. 1).

$$D\ (nm) = k\lambda/\beta \cos\theta \tag{1}$$

I was using the 'Scherrer equation' (Eq. 2), from the total width to the half maximum, the size of Ag. NPs can be determined.

$$\tau = k\lambda/\beta \cos\theta \tag{2}$$

where 'τ' (tau) is the mean size of the crystalline domain, which may be equal to grain size, 'k' is a dimensionless shape factor whose value is nearly equal to 0.9, but varies with the actual shape of the crystallite, λ is the wavelength of X-rays and β is the line broadening at half the maximum intensity (FWHM) in radians[13].

Scanning electron microscopy (SEM–EDX). Morphology of Ag. NPs were examined by using SEM ZEISS SEM (Germany) with a magnification (Max); 300,000X and resolving Power (Max); 2.3 nm that contains information about the surface topography and composition of the sample. The Ag. NPs were suspended in deionized water with a concentration of 1 mg mL^{-1} and sonicated using a sonicate bath. The sonicated stock solution (1 mg mL^{-1}) was diluted 20 times to measure the size of Ag. NPs. Then the sonicated aqueous solution was dried by taking one drop of it on a glass plate. Finally, the sample was placed on a carbon-coated copper grid, and images were taken[2,3,45]. The Oxford-EDS system (UK) was used to conduct energy dispersive X-rays (EDX) spectrometry on the ACE and Ag. NPs.

Transmission electron microscopy (TEM). The microstructure and particle size of the Ag. NPs were studied using TEM (FEI. Tecnai G2 F20, USA). The sample was dissolved in ethanol and sonicated to disperse. The pieces were then coated in carbon films, and images were taken[20].

DRS. For the diffuse reflection spectroscopy (DRS) of the Ag. NPs, the absorption spectra of biosynthesized NPs can be calculated by using Tauc's relation (Eq. 3) to determine the band energy of AgNPs.

$$(ahv)^2 = B(hv - E_{cb}) \tag{3}$$

In this equation "α" signifies the absorption coefficient and "B" is a constant. The terms hυ represents the photon energy and E_{cb} signifies the band energy. The values of band gap energy can be determined from the linear part of the curve (between $(h\upsilon)^2$ versus hυ).

N_2 adsorption/desorption isotherms (BET). The surface area and pore volume of Ag. NPs were measured at 77 K using the Brunauer–Emmett–Teller (BET) method.

XPS analysis. X-ray photoelectron spectroscopy (XPS) with a monochromatic Al Kα excitation source (VG Scientific ESCALAB220i-XL). Following Shirley background subtraction, CasaXPS software was used to do quantitative analysis of XPS data. Using a PHI5000 VersaProbeIII (Japan) analyser, all XPS data were compared to a standard binding energy of C1s of 284.5 eV (Fig. 8).

Bioassays of Ag. NPs. Bacterial strains, namely *Staphylococcus aureus* (gram-positive), *Proteus vulgaris* (gram-negative), *Agrobacterium tumefaciens* (gram-negative), and *Escherichia coli* (gram-negative), were used for the antibacterial activity Ag. NPs and ACE of *P. lanceolata*. These bacterial species were cultured for 24 h in the Petri dishes in the nutrient broth medium using up to 20 mL of melted and cooled nutrient agar[7]. The four tested species were simmered over the nutrient agar media, the ACE, and Ag. NPs were placed in the well over the medium, already developed using sterile borer. 100 µL of each 10, 50, and 100 µg mL^{-1} concentration of Ag. NPs were loaded for each well. Furthermore, the effects of ACE and Ag. NPs were studied as a function of time in fixed volumes of bacterial strain cell morphology, and a parallel bacterial inhibition was observed on the solid agar nutrient substrate. The percent inhibition zone was recorded for each concentration, and the LD_{50} and IC_{50} value was determined from the percent inhibition. As a reference, ampicillin was used[46].

For antioxidant activity, the DPPH radical scavenging analysis, hydrogen atom or electron donation abilities of the corresponding extract (ACE, Ag. NPs), and ascorbic acid (standard drug) was carried out through antioxidant action and IC_{50} was also calculated. Then layer chromatography was done for the Ag. NPs and observed before and after DPPH spray. A stable free radical at 517 nm using DPPH was used to evaluate the radical scavenging activities of the ACE and Ag. NPs. It is reduced due to H or electron donation by 1,1-diphenyl-2-picrylhydrazyl,

RETRACTED ARTICLE

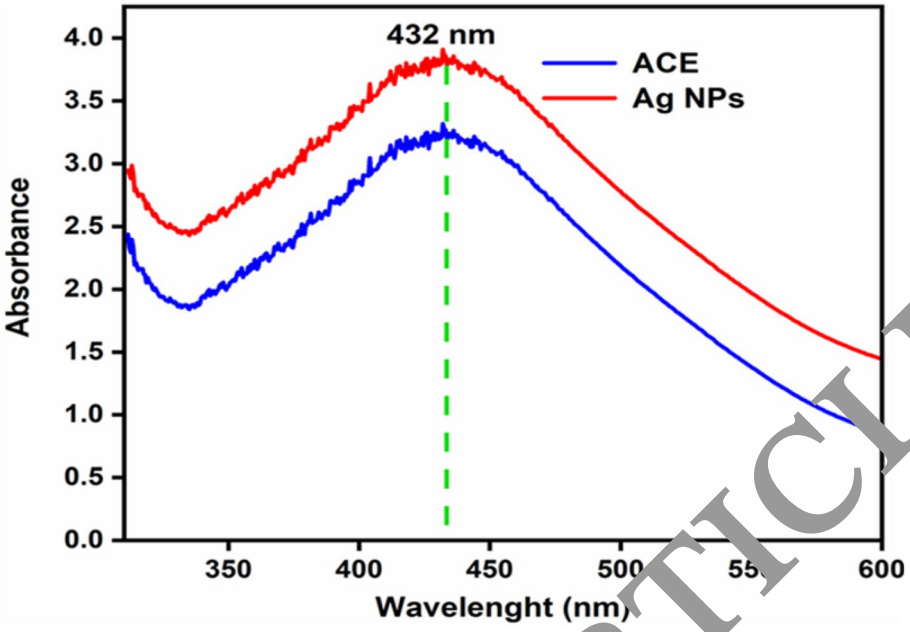

Figure 2. UV–visible absorption spectra of ACE and Ag. NPs of *Plantago lanceolata*.

whose color changes from violet to orange-yellow. The experiments were conducted in triplicate. Briefly, 1 mL solution of DPPH (1 mM) prepared in methanol was mixed with 3 mL samples (Ag. NPs each containing 10, 50, and 100 µg mL^{-1} and ACE). The solutions were stored for 30 min in the dark and the absorption was estimated at 517 nm[47].

Complies with international, national and/or institutional guidelines.. Experimental research and field studies on plants (either cultivated or wild), comply with relevant institutional, national, and international guidelines and legislation. All plant studies (*Plantago lanceolata*) were carried out in accordance with relevant institutional, national or international guidelines or regulation.

Permissions or licenses. The *Plantago lanceolata* was collected from the Mansehra (73°20′8.6″ E, 34°37′35.99″ N), after taking permission from Forestry, Environmental and Wildlife, Khyber Pakhtunkhwa, Pakistan.

Identification of the plant material. Before collection, the plant was identified by Dr. Hanif Khan (Taxonomist), using the standard protocol at the Department of Life Science, Northwest University, Xi'an, China.

Ethics approval and consent to participate. We all declare that manuscripts reporting studies do not involve any human participants, human data, or human tissue. So, it is not applicable.

Results and discussion

Silver nanoparticles. Green biosynthesis of nanoscale materials by biological materials was promoted to reduce toxic component production[6]. Efforts were made to test *P. lanceolata* for NPs synthesis and its activity[3]. The development of Ag. NPs of comparable particle size were observed by the surface plasmon resonance (SPR). Color shift was visual proof for converting Ag^+ ions of $AgCl_2$ into Ag. NPs with A.C.E. Ag. NPs had dark yellowish-brown color in an aqueous solution due to the surface plasmon resonance phenomena. After combining aqueous fraction and $AgCl_2$ colorless solutions in a 1:1 ratio, the color change due to Ag's oxidation in NPs[48]. The color strength improved over time, and after 4 h of constant stirring, the color of the mixture turned reddish-brown[49–52].

Characterization of Ag. NPs. UV–Vis's spectrum was used as a confirmation tool along with color change for the synthesis of Ag. NPs. The efficient synthesis was achieved at a 1:1 ratio with the reddish-brown color appearance[53]. At wavelength 432 nm, the UV–Vis spectrum gave maximum absorbance (Fig. 2), matching the Ag. NPs wavelength. The resonance peak of Ag. NPs occurring around this area has been recognized by numerous studies[54].

The Ag. NPs, FT-IR spectrum is presented in Fig. 3. Plant ACE contains tannins, terpenes, anthraquinone, glycosides, sugar reducers, phlobatannins, phenolic acid, flavonoids, emodin, saponins, all of which are essential in the synthesis of Ag. NPs[53]. Certain compounds are involved in the reduction of Ag and Au ions to their respective NPs. The FT-IR confirmed the characterization of Ag. NPs of *P. lanceolata* for the ACE and showed peaks at 3350.23 cm^{-1} for OH^- bond stretching, at 1635.33 cm^{-1} indicated C=O stretching, and at 557.51 cm^{-1}

RETRACTED ARTICLE

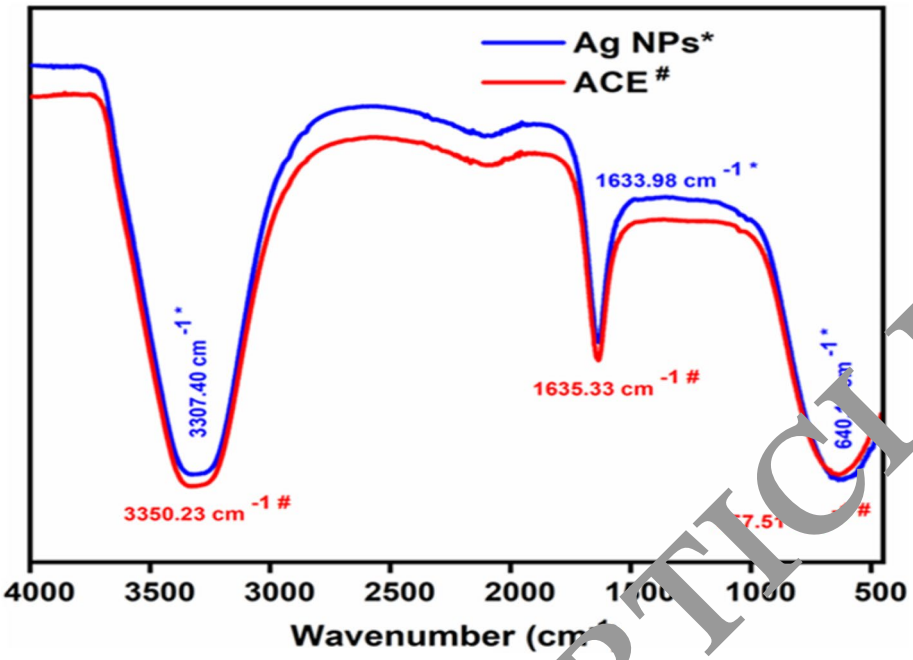

Figure 3. The ATR-FTIR spectra of ACE and Ag. NPs of *Pla*[illegible]*o lanceolata*.

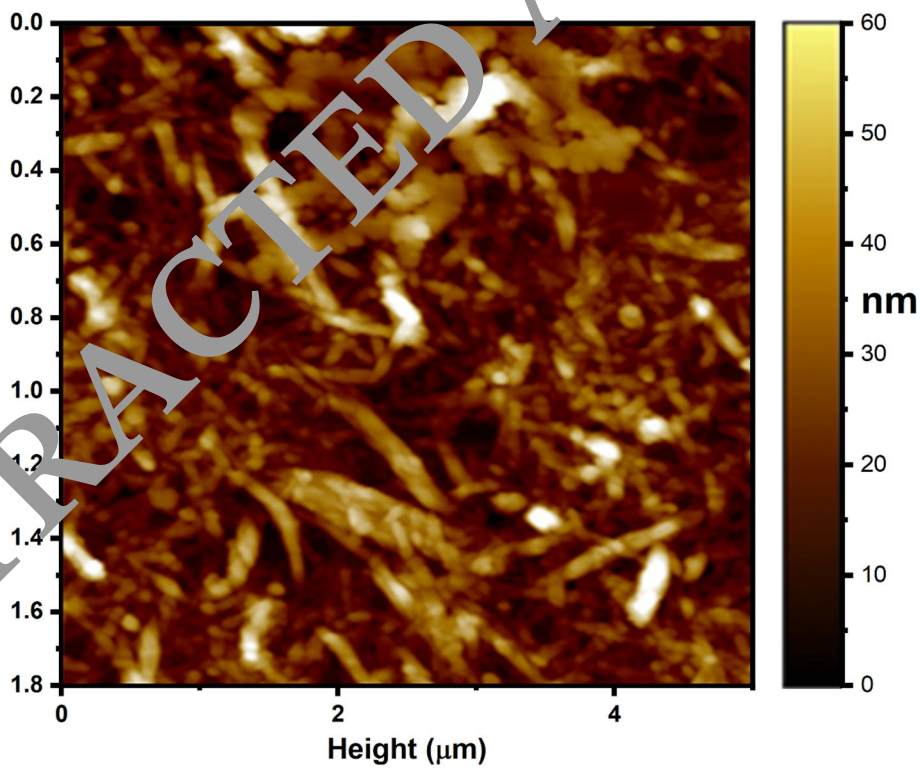

Figure 4. AFM analysis of Ag. NPs.

RETRACTED ARTICLE

showed the existence of C-H deformation. The FT-IR band showed broadening of peaks at 3307.40, 16633.98, and 640.15 cm^{-1} after reducing Ag^{+} ions (synthesis of Ag. NPs), indicating the contribution of these groups (OH^{-}, C=O, and C-H, respectively) in the synthesis of Ag. NPs[22,45].

The design, morphology and size of the orchestrated silver nanoparticles were described by the AFM pictures. Figure 4 shows parallel AFM pictures of biofunctionalized Ag. NPs. The resultant silver nanoparticle pictures

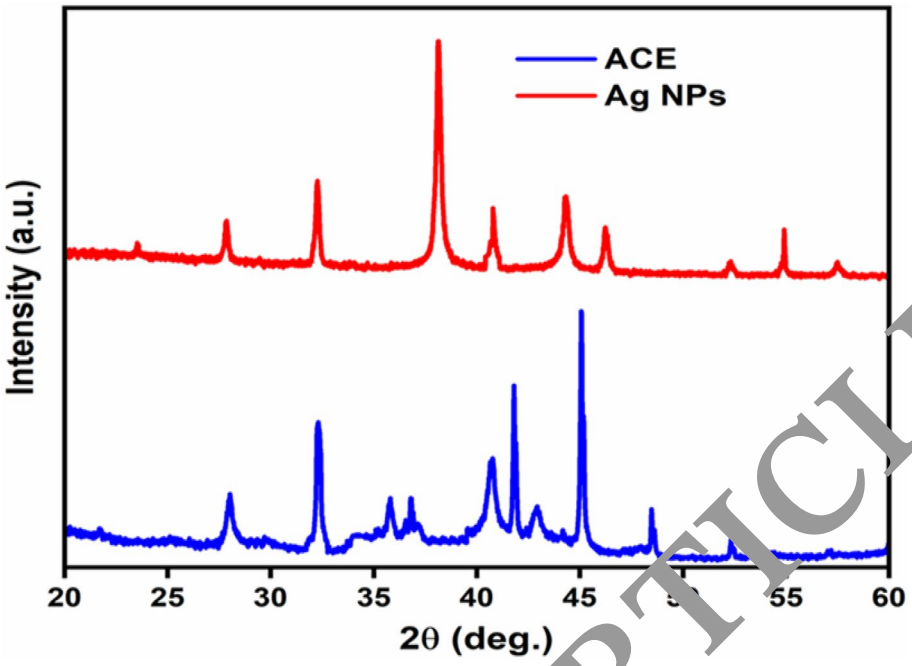

Figure 5. X-ray diffraction (XRD) of ACE and Ag. NPs of *Plantago lanceolata*.

RETRACTED ARTICLE

were seen as circular fit. The molecule size of the Ag. NPs was observed to be 55 nm and is additionally used to check that the Ag. NPs were pretty much homogenous in size.

The XRD pattern of Ag. NPs are shown in (Fig. 5). The indexing process was done in the first step, and the miller indices were assigned to each peak. Entire reflection peaks corresponded to Ag. NPs with face-centered cubic symmetry[53]. The high intensity of peaks showed that the Ag. NPs were highly crystalline[15]. The diffraction pattern of Ag. NPs indicated peaks at 23.5°, 27.83°, 38.23°, 44.25°, 46.23°, 54.80°and 57.50° of face-centered cubic pure Ag. NPs (JCPDS 76-1393)[55]. It verified that the Ag. NPs' principal constituent was Ag metal. The calculated size of Ag. NPs was 26 nm at 2θ = 27.70°, 26.5 nm at 2θ = 32.10° and 28 nm at 2θ = 46.10°[55]. The particle size obtained from the XRD plot using (Eq. 2) is well-matched with the TEM micrograph particle size; powder XRD confirmed the size of the Ag. NPs. The spherical shape, mean particle size of 30 ± 4 nm, non-uniform distribution, and aggregation of NPs with time were seen by XRD analysis[56]. The small size difference indicated that the particles were polycrystalline, while single crystals displayed a wide variety of sizes[57].

SEM was used to describe the morphology of the synthesized Ag. NPs[7]. SEM analysis showed the spherical shape and average size range 30 ± 4 nm, though the size of few particles was either large or very small (Fig. 6a,b)[5]. The SEM analysis also showed a non-uniform distribution of Ag. NPs. Morphology of Ag. NPs depend upon the association of organic compounds with Ag due to the reduction and confirmed the organic group in the ACE[20]. The TEM image of Ag. NPs indicated a slight variation in both shape and size[58]. The analysis also showed aggregations of NPs and physical interaction, which might be attributed to biomolecules (Fig. 6c,d,e). The morphology of the NPs was inconsistent, but the spherical structure was dominant, and the mean size of the NPs ranged between 26 and 34 nm, which was also confirmed SEM[4].

The EDX indicated the weight percent (54.87%) of the element in Ag. NPs (Fig. 6f)[59]. The carbon, oxygen, chlorine, and Ag were 22.91, 17.25, 4.97, and 54.87. It indicated the higher content of Ag in the Ag. NPs.

The DRS absorption spectra of biosynthesized Ag. NPs can be calculated by using Tauc's relation (Eq. 3) to determine the band energy of Ag. NPs. In this equation "α" signifies the absorption coefficient and "B" is a constant. The terms hυ represents the photon energy and E_g signifies the band energy. The values of band gap energy can be determined from the linear part of the curve (between $(h\upsilon)^2$ versus hυ). The calculated amount of band gap energy was 2.34 eV for Ag. NPs as shown in (Fig. 7)[60].

BET technique was used to find out the surface areas of the Ag. NPs. The physical and chemical properties of NPs must be characterized in order to ensure the repeatability of toxicology investigations and to learn how the physical and chemical properties of NPs impact their biological effects. Nitrogen (N_2) gas is used in the BET surface area analysis of Ag. NPs. The reason is that N_2 gas is available in pure form and it has very interaction with solid Ag. NPs. The BET adsorption isotherms for Ag. NPs is described in (Fig. 8). The BET surface area, total pore volume and average pore radius are mentioned that the Ag. NPs having the Maximum surface area was found for 7.38m^2/g with total pore volume as 0.0389 mL/g and average pore radius as 1.0964 nm in this case. The highest catalytic activity of Ag. NPs could be attributed in terms of their maximum surface area7.38m^2/g with total pore volume as 0.0389 mL/g and average pore radius as 1.0964 nm[61].

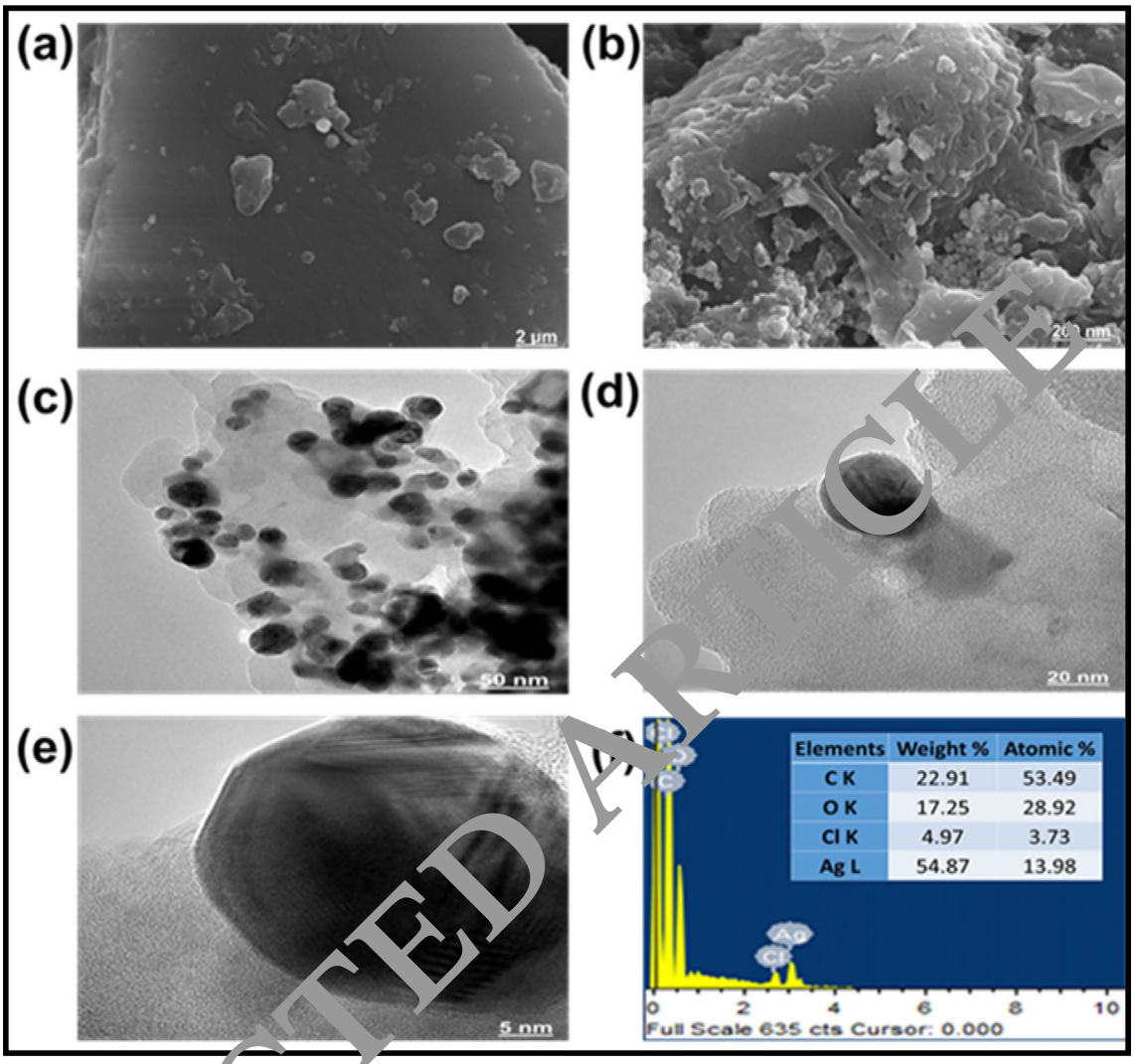

Figure 6. SEM, EDX and TEM analysis of Ag. NPs. The SEM images of the Ag. NPs at 2 µm (**a**) and 200 µm (**b**). TEM images were analyzed at 50 nm (**c**), 20 nm (**d**), and 5 nm (**e**), the EDX spectrum (**f**), indicating the weight percent of the element in Ag. NPs.

RETRACTED ARTICLE

XPS studies. XPS sequencing was used to identify the defining characteristics in the synthesized materials (Fig. 9a). On every analysis, low-resolution scans with 1 eV of step energy were acquired throughout an overall energy continuum of 0–1361 eV. With the same binding energies of Ag metal and silver oxide, determining Ag ions using the XPS approach is indeed particularly sensitive for researchers. The $Ag3d_{5/2}$ peak, which indicates Ag, Ag_2O, and AgO, had binding energy of 367.898–374.33. Ag $3d_{3/2}$ was responsible for the smaller energy peak, while Ag $3d_{5/2}$ was responsible for the enhanced energy peak (Fig. 9b).

The binding energies from 284.14 to 284.53 (Fig. 9c) revealed the presence of C1s with the lower energy for adventitious carbon and high energy for carbonate carbon.

The presence of adsorbed oxygen species was indicated by the peak at an energy value of 532.46–532.89 eV (Fig. 9d).

Antibacterial activity. The antimicrobial activity of Ag. NPs were enhanced by the phytonutrients that preserved them and the increased antibacterial potency of Ag. NPs is due to the macromolecules and surface area. The small size, dispersion, and spherical morphology may be correlated with the antibacterial viability of the Ag. NPs, which offer a wide surface for maximal contact with bacteria, resulting in even more damage than larger particle size[62]. The antibacterial activity of both ACE and Ag. NPs were tested against the four bacterial species (Fig. 10)[63]. Effects of Ag. NPs as a time feature in fixed amounts of cell morphology of bacterial strains were analyzed. The corresponding bacterial count was also determined on the solid agar nutrient media[47]. Besides, each of the tested bacterial strains was significantly reduced compared with control (Ampicillin). The result is associated with the area of the inhibition assay. The Ag. NPs showed very significant activity against all the four selected bacterial strains (*P. vulgaris* of LD_{50} 726.46, *A. tumefaciens* of LD_{50} 332.87, *E. coli* of LD_{50} 45.66, and *S. aureus* of LD_{50} 45.54) as compared to ACE, showing the highest resistance of *P. vulgaris* among all the

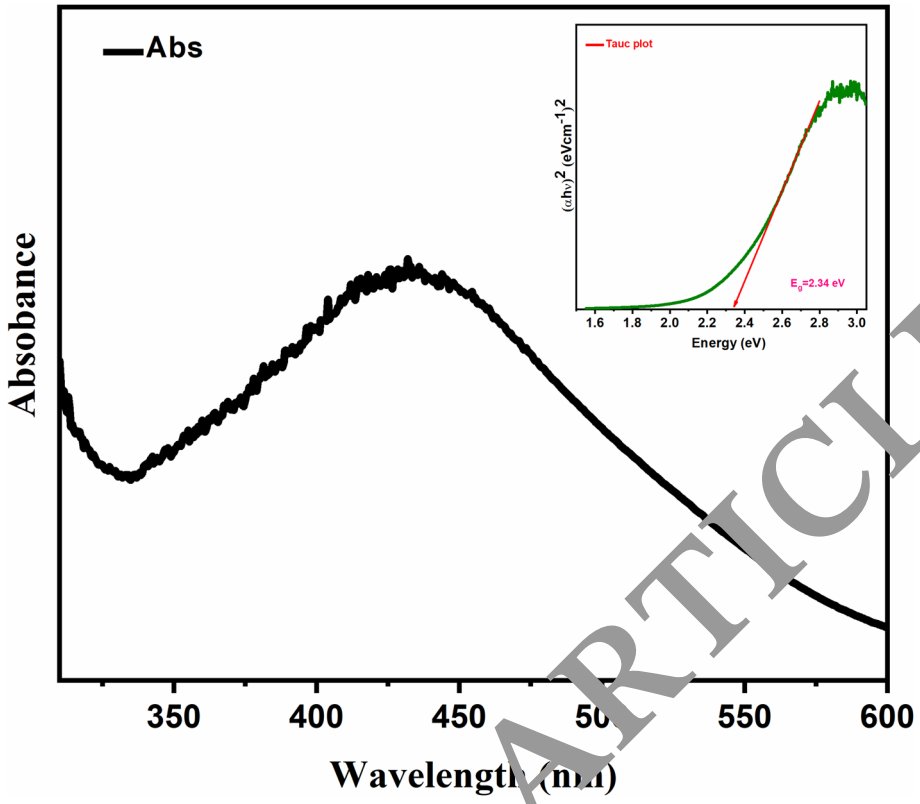

Figure 7. DRS of Ag. NPs showing E_g = 2.34 eV.

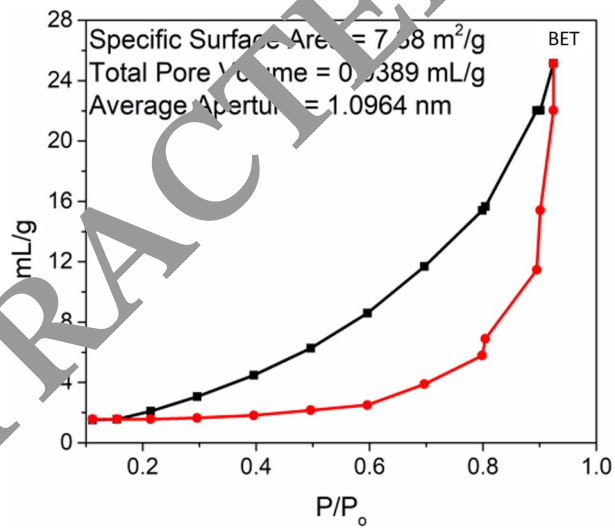

Figure 8. Nitrogen adsorption/desorption isotherms of Ag. NPs (BET).

RETRACTED ARTICLE

four strains[30]. Also show good results for IC_{50} values for (*P. vulgaris* (55.78 ± 1.01), *A. tumefaciens* (08.02 ± 0.68), *E. coli* (11.68 ± 1.42) and *S. aureus* (12.34 ± 1.35) (Table 1). Clinical trials have demonstrated that the association of Ag^+ ions with NPs has antimicrobial effects[53]. Numerous factors are linked primarily with the antimicrobial property of Ag. NPs, which include (i) the overproduction of reactive oxygen species like superoxide (O^{2-}) and OH^-, (ii) the existence of Ag^+ ions in Ag. NPs that form bacterial protein sulfhydryl groups, and (iii) the release of Ag^+ ions by Ag. NPs that infiltrate the cellular structure and destroy bacteria[62].

Ag. NPs have a large surface area and smaller size, allowing broad interaction with the bacteria cell wall and toxic to cytoplasmic content in a systematic way[45]. The redox study indicates that Ag^+ ions emitted from the Ag. NPs surface is responsible for their antibacterial assay[19]. The thin peptidoglycan framework of bacteria ensures

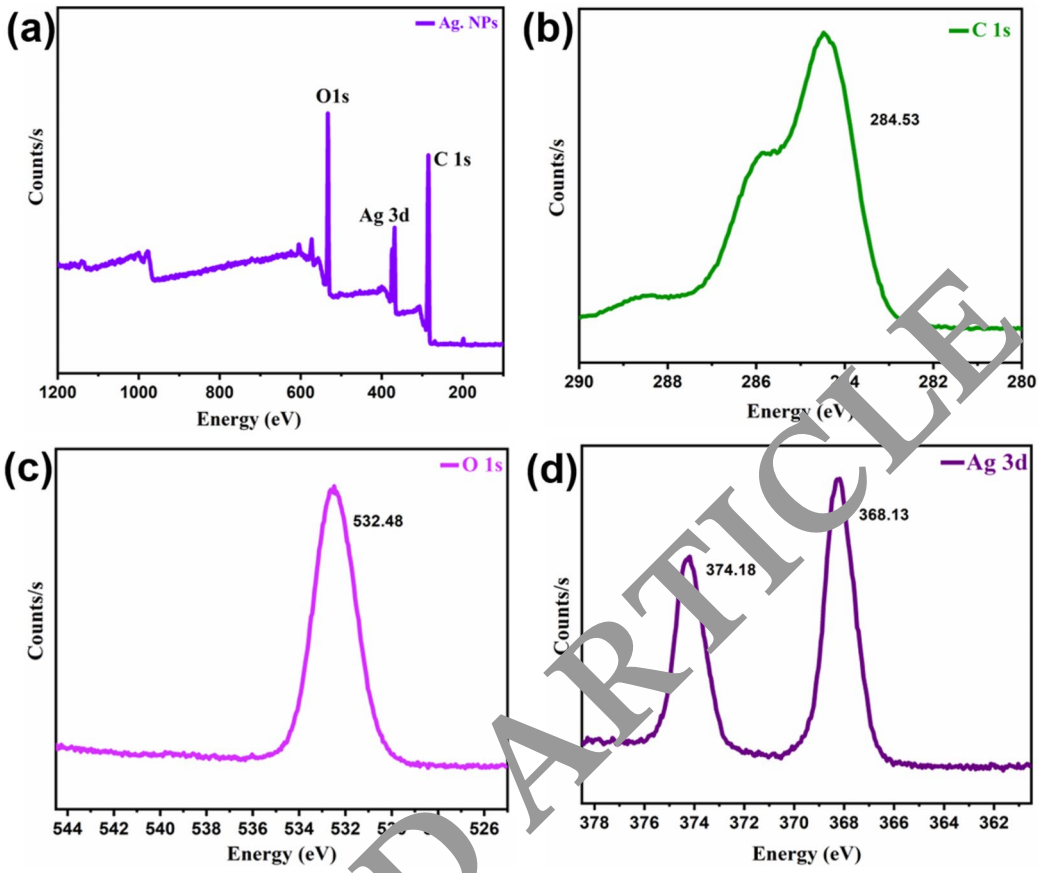

Figure 9. XPS studies of Ag. NPs.

that the Ag. NPs can directly enter the cytoplasm and interact with the cell membrane, causing damage to membranous protein[57]. Also, Ag. NPs posed significant antibacterial efficacy against *Escherichia coli*. *Escherichia coli* are much more susceptible to Ag. NPs than *Agrobacterium tumefaciens*, *Proteus vulgaris*, and *Staphylococcus aureus*. The smaller NPs have a reduced interparticle gap and an increased number of unit cells measured from the XRD measurements impacting the electron density at the surface of the NPs[64]. Thus, Ag. NPs demonstrated the most vital antimicrobial property based on our findings which indicate that the choice of *P. lanceolate* is best for the synthesis of Ag. NPs.

Antioxidant activity of Ag. NPs. The DPPH scavenging assay was used to assess the antioxidant function of the ACE and Ag. NPs[65]. Both samples were applied at different concentrations (10–100 μg mL^{-1}). The thin layer chromatography of DPPH identified zones with varying values of retention factor (rf)[66]. ACE and Ag. NPs have substantial DPPH free radical scavenging activities to estimate their antioxidant ability, which is proven relative to the standard antioxidants[44]. The ACE and Ag. NPs exhibited maximum antioxidant capacity of 62.43 ± 2.4 and 16.85 ± 0.4 at 100 μg mL^{-1}, respectively) compared to control (69.60 ± 1.1 at 100 μg mL^{-1})[67]. Also gave results for IC_{50} values for ACE and Ag. NPs 369.5 ± 13.42 and 159.5 ± 10.52 respectively regarding DPPH radicals (Table 2). The findings revealed that the antioxidant potential of both ACE and Ag. NPs increased with higher concentration. However, ACE and Ag. NPs gave slightly lower activity than ascorbic acid/reference (Fig. 11). These activities were in line with the previous reports regarding *P. lanceolata* and other species[68].

Plantago species have immune-stimulating properties and helping the animal's defense system; therefore, few antibiotic growth agents might be required. *Plantago lanceolata* phytochemical analysis indicated the presence of reducing sugar, glycoside, anthraquinone, and tannins[69]. This shows that *Plantago lanceolata*, collected from Mansehra, was reported for the first time for its Ag. NPs synthesis and antioxidant activities. The high scavenging activity of the ACE and Ag. NPs could be ascribed to these compounds that may exert a synergistic effect[70]. It is evident from the current research work that both ACE and Ag. NPs should be considered as a good antioxidant[41,55,71,72].

Conclusion

The resultant silver nanoparticle pictures were seen as circular fit. The molecule size of the Ag. NPs was observed to be 55 nm and is additionally used to check that the Ag. NPs were pretty much homogenous in size. Thusly, this response pathway fulfils every one of the states of a 100% green chemical process. The measure of plant material is found to assume a basic part in controlling the size of a lot of dispersity of nanoparticles, so more

RETRACTED ARTICLE

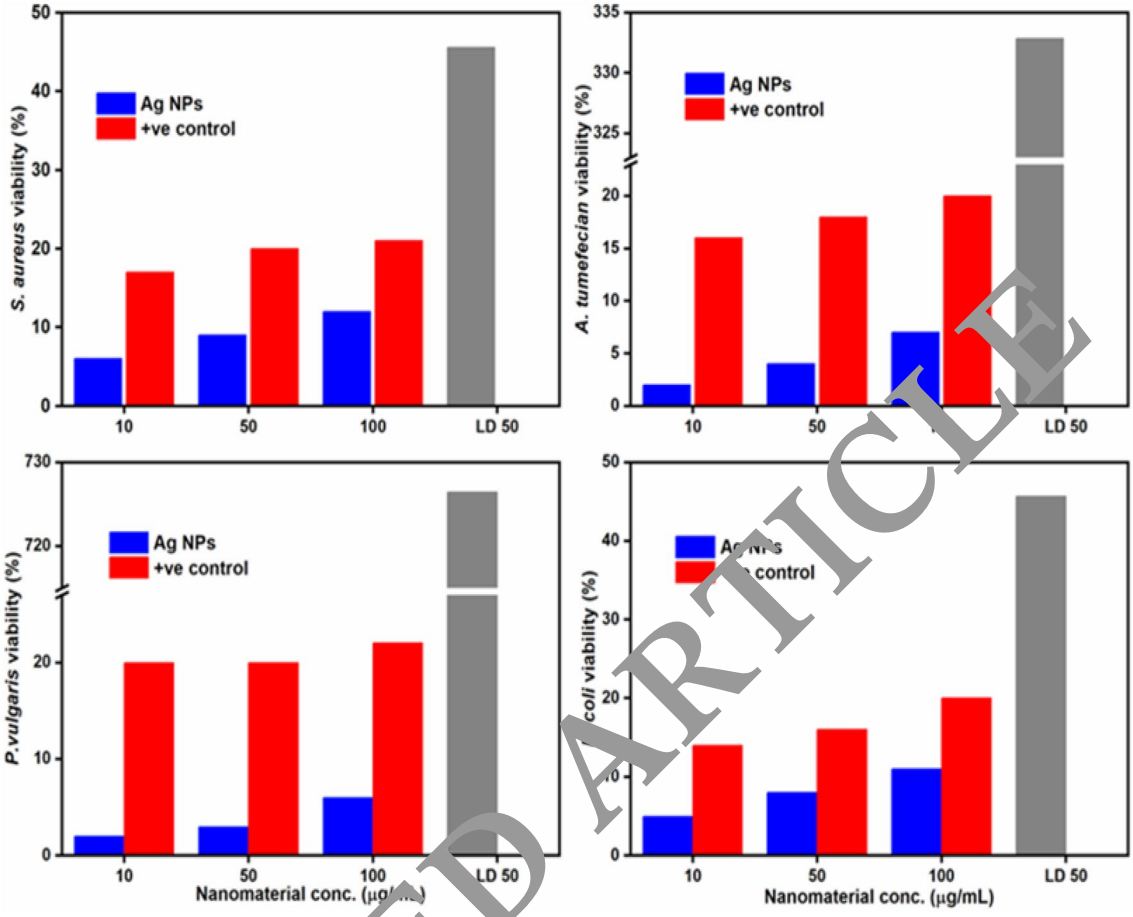

Figure 10. Antibacterial activity of the ACE and Ag. NPs of *Plantago lanceolata* LD_{50} is concentration causing 50% inhibition.

Bacterial specie	LD_{50} [a] (mg/L)	IC_{50} [a] (µg/mL)
A. tumefaciens	726.46	08.02 ± 0.68
P. vulgaris	332.87	55.78 ± 1.01
S. aureus	45.66	12.34 ± 1.35
E. coli	45.54	11.68 ± 1.42
Ampicillin[b]	12.28	32

Table 1. Antioxidant activity (DPPH) and IC_{50} value in ACE and Ag. NPs. [a]IC_{50} = Signifies the means (± standard error) of 3 equivalent amounts ($p < 0.05$). [b]Reference.

Compounds	DPPH[a] (µg/mL)	IC_{50} [a] (µg/mL)
ACE	62.43 ± 2.4	369.5 ± 13.42
Ag. NPs	16.85 ± 0.4	159.5 ± 10.52
Ascorbic acid[b]	69.60 ± 1.1	66.12 ± 11.29

Table 2. Antibacterial activity of the ACE and Ag. NPs of *P. lanceolata* LD_{50} and IC_{50} is concentration causing 50% inhibition. [a]IC_{50} = Signifies the means (± standard error) of 3 equivalent amounts ($p < 0.05$). [b]Reference.

modest silver nanoparticles and limited size. The size of the Ag. NPs depend upon organic macromolecules found in ACE (phenolic acid and flavonoids). High antibacterial activity for Ag. NPs against *Proteus vulgaris*, *Agrobacterium tumefecian*, *Staphylococcus aureus,* and *Escherichia coli* showed LD_{50} values as 726.46, 332.87, 45.66, and 45.54 mg L^{-1}, respectively. The DPPH of ACE and Ag. NPs gave a maximum value of 62.43 ± 2.4 and

RETRACTED ARTICLE

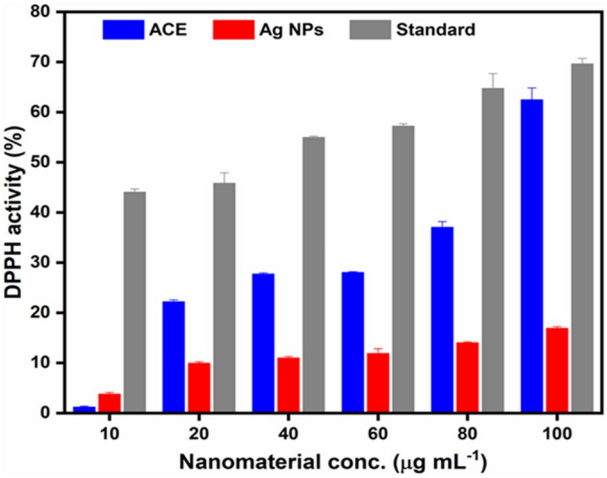

Figure 11. DPPH assay of the ACE and Ag. NPs of *Plantago lanceolata*.

16.85 ± 0.4 at 100 μg L^{-1}, respectively, showing an increase with high concentration. Finally, *P. lanceolata* extract and its Ag. NPs might be the best option for therapeutic and medical applications.

Received: 23 June 2021; Accepted: 6 October 2021
Published online: 21 October 2021

References

1. Shanmugapriya, K. & Kang, H. W. Engineering pharmaceutical nanocarriers for photodynamic therapy on wound healing. *Mater. Sci. Eng.: C* **105**, 110110 (2019).
2. Shu, M. *et al.* Biosynthesis and antibacterial activity of silver nanoparticles using yeast extract as reducing and capping agents. *Nanoscale Res. Lett.* https://doi.org/10.1186/s11671-019-3244-z (2020).
3. Velusamy, P., Das, J., Pachaiappan, R., Vaseeharan, B. & Pandian, K. Greener approach for synthesis of antibacterial silver nanoparticles using aqueous solution of neem gum (*Indirachta indica* L.). *Ind. Crops Prod.* **66**, 103–109 (2015).
4. Varadavenkatesan, T., Selvaraj, R. & Vinayagam, R. Dye degradation and antibacterial activity of green synthesized silver nanoparticles using *Ipomoea digitata* L. flower extract. *Int. J. Environ. Sci. Technol.* **16**, 2395–2404 (2019).
5. Vishwasrao, C., Momin, M. & Ananthanarayan, L. Green synthesis of silver nanoparticles using sapota fruit waste and evaluation of their antimicrobial activity. *Waste Biomass Valorization* **10**, 2353–2363 (2019).
6. Bharathi, D., Josebin, M. D., Vasantharaj, S. & Bhuvaneshwari, V. Biosynthesis of silver nanoparticles using stem bark extracts of *Diospyros montana* and their antioxidant and antibacterial activities. *J. Nanostruct. Chem.* **8**, 83–92 (2018).
7. Rai, M. *et al.* Broad-spectrum bioactivities of silver nanoparticles: the emerging trends and future prospects. *Appl. Microbiol. Biotechnol.* **98**, 1951–1961 (2014).
8. Daniel, S. K., Vasanthi, G., Subramanian, N., Nehru, K. & Sivakumar, M. Biosynthesis of Cu, ZVI, and Ag nanoparticles using *Dodonaea viscosa* extract for antibacterial activity against human pathogens. *J. Nanopart. Res.* **15**, 1319 (2013).
9. Baláž, M. [Corrigendum to "Bio-mechanochemical synthesis of silver nanoparticles with antibacterial activity" [Adv. Powder Technol. 28(12) (2017) 3307–3312]. *Adv. Powder Technol.* **30**, 219–220. https://doi.org/10.1016/j.apt.2018.11.018 (2019).
10. Vigo, E., Cepeda, A., Gualillo, O. & Perez-Fernandez, R. In-vitro anti-inflammatory activity of Pinus *sylvestris* and *Plantago lanceolata* extracts: effect on inducible NOS, COX-1, COX-2 and their products in J774A. 1 murine macrophages. *J. Pharm. Pharmacol.* **57**, 383–391 (2005).
11. Dos Santos, C. A. *et al.* Silver nanoparticles: therapeutical uses, toxicity, and safety issues. *J. Pharm. Sci.* **103**, 1931–1944 (2014).
12. Lizzo, M. *et al.* Antioxidant and antibacterial activities on foodborne pathogens of *Artocarpus heterophyllus* Lam. (Moraceae) leaves extracts. *J. Food Sci.* **75**, M291–M295 (2010).
13. Nayagam, V., Gabriel, M. & Palanisamy, K. Green synthesis of silver nanoparticles mediated by *Coccinia grandis* and *Phyllanthus emblica*: a comparative comprehension. *Appl. Nanosci.* **8**, 205–219 (2018).
14. Ezer, N. & Arisan, Ö. M. Folk medicines in Merzifon (Amasya, Turkey). *Turk. J. Bot.* **30**, 223–230 (2006).
15. Srikar, S. K., Giri, D. D., Pal, D. B., Mishra, P. K. & Upadhyay, S. N. Green synthesis of silver nanoparticles: A review. *Green Sustain. Chem.* **6**, 34 (2016).
16. Beara, I. N. *et al.* Comparative analysis of phenolic profile, antioxidant, anti-inflammatory and cytotoxic activity of two closely-related Plantain species: *Plantago altissima* L. and *Plantago lanceolata* L. *LWT-Food Sci. Technol.* **47**, 64–70 (2012).
17. Dalar, A., Türker, M. & Konczak, I. Antioxidant capacity and phenolic constituents of *Malva neglecta* Wallr. and *Plantago lanceolata* L. from Eastern Anatolia Region of Turkey. *J. Herb. Med.* **2**, 42–51 (2012).
18. Henglein, A. Colloidal silver nanoparticles: photochemical preparation and interaction with O2, CCl4, and some metal ions. *Chem. Mater.* **10**, 444–450 (1998).
19. Song, J. Y. & Kim, B. S. Rapid biological synthesis of silver nanoparticles using plant leaf extracts. *Bioprocess Biosyst. Eng.* **32**, 79 (2009).
20. Singhal, G., Bhavesh, R., Kasariya, K., Sharma, A. R. & Singh, R. P. Biosynthesis of silver nanoparticles using *Ocimum sanctum* (Tulsi) leaf extract and screening its antimicrobial activity. *J. Nanopart. Res.* **13**, 2981–2988 (2011).
21. Shahverdi, A. R., Minaeian, S., Shahverdi, H. R., Jamalifar, H. & Nohi, A.-A. Rapid synthesis of silver nanoparticles using culture supernatants of Enterobacteria: A novel biological approach. *Process Biochem.* **42**, 919–923 (2007).
22. Sanghi, R. & Verma, P. Biomimetic synthesis and characterisation of protein capped silver nanoparticles. *Biores. Technol.* **100**, 501–504 (2009).
23. Kumar, B., Smita, K., Cumbal, L. & Debut, A. Synthesis of silver nanoparticles using Sacha inchi (*Plukenetia volubilis* L.) leaf extracts. *Saudi J. Biol. Sci.* **21**, 605–609 (2014).

RETRACTED ARTICLE

24. Ahmed, E.-H.M., Nour, B. Y., Mohammed, Y. G. & Khalid, H. S. Antiplasmodial activity of some medicinal plants used in Sudanese folk-medicine. *Environ. Health Insights (EHI)* **4**, S4108 (2010).
25. Roopan, S. M. *et al.* Low-cost and eco-friendly phyto-synthesis of silver nanoparticles using *Cocos nucifera* coir extract and its larvicidal activity. *Ind. Crops Prod.* **43**, 631–635 (2013).
26. Gan, P. P. & Li, S. F. Y. Potential of plant as a biological factory to synthesize gold and silver nanoparticles and their applications. *Rev. Environ. Sci. Bio/Technol.* **11**, 169–206 (2012).
27. Girase, B., Depan, D., Shah, J., Xu, W. & Misra, R. Silver–clay nanohybrid structure for effective and diffusion-controlled antimicrobial activity. *Mater. Sci. Eng.: C* **31**, 1759–1766 (2011).
28. Kelly, F. M. & Johnston, J. H. Colored and functional silver nanoparticle–wool fiber composites. *ACS Appl. Mater. Interfaces.* **3**, 1083–1092 (2011).
29. Dancer, S. J. Hospital cleaning in the 21st century. *Eur. J. Clin. Microbiol. Infect. Dis.* **30**, 1473–1481 (2011).
30. Gopinath, K., Gowri, S. & Arumugam, A. Phytosynthesis of silver nanoparticles using *Pterocarpus santalinus* leaf extract and their antibacterial properties. *J. Nanostruct. Chem.* **3**, 68 (2013).
31. Bajer, T. *et al.* Chemical composition of essential oils from *Plantago lanceolata* L. leaves extracted by hydrodistillation. *J. Food Sci. Technol.* **53**, 1576–1584 (2016).
32. Usha, B., Venkataraman, G. & Parida, A. Heavy metal and abiotic stress inducible metallothionein isoforms from *Prosopis juliflora* (SW) DC show differences in binding to heavy metals in vitro. *Mol. Genet. Genom.* **281**, 99–108 (2009).
33. Navrátilová, M. *et al.* Pharmaceuticals in environment: the effect of ivermectin on ribwort plantain (*Plantago lanceolata* L.). *Environ. Sci. Pollut. Res.* **27**, 31202–31210 (2020).
34. Sargin, S. A. Ethnobotanical survey of medicinal plants in Bozyazı district of Mersin, Turkey. *J. Ethnopharmacol.* **173**, 105–126 (2015).
35. Makarov, V. *et al.* "Green" nanotechnologies: synthesis of metal nanoparticles using plants. *Acta Nat. (англоязычная версия)* **6**, 35–44 (2014).
36. Mazzutti, S., Riehl, C. A., Ibañez, E. & Ferreira, S. R. Green-based methods to obtain bioactive extracts from Plantago major and *Plantago lanceolata*. *J. Supercrit. Fluids* **119**, 211–220 (2017).
37. Nemereshina, O. N., Tinkov, A. A., Gritsenko, V. A. & Nikonorov, A. A. Influence of Plantaginaceae species on *E. coli* K12 growth in vitro: Possible relation to phytochemical properties. *Pharm. Biol.* **53**, 719–724 (2015).
38. Abd-Alla, H. I. *et al.* Efficacy of extracts and iridoid glucosides from *Pentas lanceolata* on humoral and cell-mediated immune response of viral vaccine. *Med. Chem. Res.* **26**, 2196–2204 (2017).
39. Sõukand, R. & Pieroni, A. The importance of a border: medicinal, culinary, and wild food ethnobotany of the Hutsuls living on the Romanian and Ukrainian sides of Bukovina. *J. Ethnopharmacol.* **185**, 179–211 (2016).
40. Bachheti, R., Godebo, Y., Bachheti, A., Yassin, M. O. & Husen, A. Rose-based fabrication of metal/metal-oxide nanomaterials and their various applications. In *Nanomaterials for Agriculture and Forestry Applications* (eds Husen, A. & Jawaid, M.) 135–166 (Elsevier, 2020).
41. Ahmad, M. *et al.* An ethnobotanical study of medicinal plants in high mountainous region of Chail valley (District Swat-Pakistan). *J. Ethnobiol. Ethnomed.* **10**, 36 (2014).
42. Izhaki, I. Emodin—A secondary metabolite with multiple ecological functions in higher plants. *New Phytol.* **155**, 205–217 (2002).
43. Mazzutti, S., Ferreira, S. R. S., Herrero, M. & Ibañez, E. Intensified aqueous-based processes to obtain bioactive extracts from Plantago major and *Plantago lanceolata*. *J. Supercrit. Fluids* **119**, 64–71 (2017).
44. Chugh, H. *et al.* Role of gold and silver nanoparticles in cancer nano-medicine. *Artif. Cells Nanomed. Biotechnol.* **46**, 1210–1220 (2018).
45. Nikaeen, G., Yousefinejad, S., Abdedi, S., Somari, F. & Mahdavinia, S. Central composite design for optimizing the biosynthesis of silver nanoparticles using Plantago major extract and investigating antibacterial, antifungal and antioxidant activity. *Sci. Rep.* **10**, 1–16 (2020).
46. Hai, R. *et al.* Influenza A (H1N9) virus gains neuraminidase inhibitor resistance without loss of in vivo virulence or transmissibility. *Nat. Commun.* **4**, 1–9 (2013).
47. Marta, B. *et al.* Designing chitosan–silver nanoparticles–graphene oxide nanohybrids with enhanced antibacterial activity against *Staphylococcus aureus*. *Colloids Surf., A* **487**, 113–120 (2015).
48. Ibrahim, M. *et al.* Acetyl and butyryl cholinesterase inhibitory sesquiterpene lactones from *Amberboa ramosa*. *Chem. Cent. J.* **7**, 116 (2013).
49. Ibrahim, H. M. Green synthesis and characterization of silver nanoparticles using banana peel extract and their antimicrobial activity against representative microorganisms. *J. Radiat. Res. Appl. Sci.* **8**, 265–275 (2015).
50. Khan, A., Saeed, K. & Khan, I. Nanoparticles: Properties, applications and toxicities. *Arab. J. Chem.* **12**, 908–931 (2019).
51. Sharma, D., Pramanik, A. & Agrawal, P. K. Evaluation of bioactive secondary metabolites from endophytic fungus *Pestalotiopsis neglecta* MGB-5510 isolated from leaves of *Cupressus torulosa* D. Don. *3 Biotech* **6**, 210 (2016).
52. [illegible] V. K., Yngard, R. A. & Lin, Y. Silver nanoparticles: green synthesis and their antimicrobial activities. *Adv. Coll. Interface. Sci.* **145**, 83–96 (2009).
53. Venkatesan, J., Kim, S.-K. & Shim, M. S. Antimicrobial, antioxidant, and anticancer activities of biosynthesized silver nanoparticles using marine algae *Ecklonia cava*. *Nanomaterials* **6**, 235 (2016).
54. Edison, T. J. I. & Sethuraman, M. Biogenic robust synthesis of silver nanoparticles using *Punica granatum* peel and its application as a green catalyst for the reduction of an anthropogenic pollutant 4-nitrophenol. *Spectrochim. Acta Part A Mol. Biomol. Spectrosc.* **104**, 262–264 (2013).
55. Nakkala, J. R., Mata, R., Bhagat, E. & Sadras, S. R. Green synthesis of silver and gold nanoparticles from *Gymnema sylvestre* leaf extract: study of antioxidant and anticancer activities. *J. Nanopart. Res.* **17**, 151 (2015).
56. Ibrahim, Y. *et al.* Unveiling fabrication and environmental remediation of MXene-based nanoarchitectures in toxic metals removal from wastewater: Strategy and mechanism. *Nanomaterials* **10**, 885 (2020).
57. Eckhardt, S. *et al.* Nanobio silver: its interactions with peptides and bacteria, and its uses in medicine. *Chem. Rev.* **113**, 4708–4754 (2013).
58. Fabiyi, O. A., Alabi, R. O. & Ansari, R. A. Nanoparticles' synthesis and their application in the management of phytonematodes: An overview. In *Management of Phytonematodes: Recent Advances and Future Challenges* (eds Ansari, R. *et al.*) 125–140 (Springer, 2020).
59. Al Aboody, M. S. Silver/silver chloride (Ag/AgCl) nanoparticles synthesized from *Azadirachta indica* lalex and its antibiofilm activity against fluconazole resistant *Candida tropicalis*. *Artif. Cells Nanomed. Biotechnol.* **47**, 2107–2113 (2019).
60. Puga, F., Navio, J. & Hidalgo, M. Enhanced UV and visible light photocatalytic properties of synthesized AgBr/SnO_2 composites. *Sep. Purif. Technol.* **257**, 117948 (2021).
61. Ghosh, S., Molla, R. A., Kayal, U., Bhaumik, A. & Islam, S. M. Ag NPs decorated on a COF in the presence of DBU as an efficient catalytic system for the synthesis of tetramic acids via CO2 fixation into propargylic amines at atmospheric pressure. *Dalton Trans.* **48**, 4657–4666 (2019).
62. Taglietti, A. *et al.* Antibacterial activity of glutathione-coated silver nanoparticles against gram positive and gram negative bacteria. *Langmuir* **28**, 8140–8148 (2012).

RETRACTED ARTICLE

63. Kannaiyan, S. & Gopal, A. Biogenic synthesized silver colloid for colorimetric sensing of dichromate ion and antidiabetic studies. *Res. Chem. Intermed.* **43**, 2693–2706 (2017).
64. Tomaino, A. *et al.* Antioxidant activity and phenolic profile of pistachio (*Pistacia vera* L., variety Bronte) seeds and skins. *Biochimie* **92**, 1115–1122 (2010).
65. Dara, P. K. *et al.* Synthesis and biochemical characterization of silver nanoparticles grafted chitosan (Chi-Ag-NPs): in vitro studies on antioxidant and antibacterial applications. *SN Appl. Sci.* **2**, 1–12 (2020).
66. Banerjee, P., Satapathy, M., Mukhopahayay, A. & Das, P. Leaf extract mediated green synthesis of silver nanoparticles from widely available Indian plants: synthesis, characterization, antimicrobial property and toxicity analysis. *Bioresour. Bioprocess.* **1**, 3 (2014).
67. Tang, S. & Zheng, J. Antibacterial activity of silver nanoparticles: Structural effects. *Adv. Healthcare Mater.* **7**, 1701503 (2018).
68. Beyene, H. D., Werkneh, A. A., Bezabh, H. K. & Ambaye, T. G. Synthesis paradigm and applications of silver nanoparticles (AgNPs), a review. *Sustain. Mater. Technol.* **13**, 18–23 (2017).
69. Adom, M. B. *et al.* Chemical constituents and medical benefits of Plantago major. *Biomed. Pharmacother.* **96**, 348–360 (2017).
70. Arshad, M. *et al.* An ethnobiological study in Kala Chitta hills of Pothwar region, Pakistan: Multinomial logit specification. *J. Ethnobiol. Ethnomed.* **10**, 13 (2014).
71. Sultan-Ud-Din, A. H., Ali, H. & Ali, H. Floristic composition and life form classes of district Shangla, Khyber Pakhtunkhwa, Pakistan. *J Bio Env Sci* **8**, 187–206 (2016).
72. Hussain, W., Ullah, M., Dastagir, G. & Badshah, L. Quantitative ethnobotanical appraisal of medicinal plants used by inhabitants of lower Kurram, Kurram agency, Pakistan. *Avicenna J. Phytomed.* **8**, 313 (2018).

Acknowledgements

The authors would like to extend their sincere appreciation to the Researchers Supporting Project number (RSP-2021/194), King Saud University, Riyadh, Saudi Arabia. This work was supported by generous grants from the National Natural Science Foundation of China (NSFC-21971204, 21622205). The calculations were performed at the chemical HPC center of NWU.

Author contributions

Concept, Z-H. G.; method, M.Z.S., S.A., W.N., H.M.H.; software, A.U.D.; validation, A.A., A.U.R and K.J.; formal analysis, M.Z.S.; investigation, K.J.; resources, S.F.S; data curation, S.S.; M.A., and F.W.; writing—original draft preparation, S.F., S.Al., and M.H.S.; writing—review and editing, S.F.; visualization, Z-H. G.; supervisor, Z-H. G.

Competing interests

The authors declare no competing interests.

Additional information

Correspondence and requests for materials should be addressed to Z.-H.G., A.U.D., S.S. or S.F.

Reprints and permissions information is available at www.nature.com/reprints.

Publisher's note Springer Nature remains neutral with regard to jurisdictional claims in published maps and institutional affiliations.

Open Access This article is licensed under a Creative Commons Attribution 4.0 International License, which permits use, sharing, adaptation, distribution and reproduction in any medium or format, as long as you give appropriate credit to the original author(s) and the source, provide a link to the Creative Commons licence, and indicate if changes were made. The images or other third party material in this article are included in the article's Creative Commons licence, unless indicated otherwise in a credit line to the material. If material is not included in the article's Creative Commons licence and your intended use is not permitted by statutory regulation or exceeds the permitted use, you will need to obtain permission directly from the copyright holder. To view a copy of this licence, visit http://creativecommons.org/licenses/by/4.0/.

© The Author(s) 2021

RETRACTED ARTICLE